Multistage vertical seismic isolation for equipment in power plants

Mohammadreza Najafi[1], Tracy C. Becker[2], Dimitrios Konstantinidis[2]

[1] Ph.D. Candidate, Department of Civil Engineering, McMaster University, Hamilton, ON, Canada.
[2] Assistant Professor, Department of Civil and Environmental Engineering, University of California, Berkeley, USA.

ABSTRACT

Isolation systems are widely recognized as beneficial for protecting both acceleration- and displacement-sensitive operational and functional components. Furthermore, adaptive isolation systems enable engineers to achieve various performance goals under multiple hazard levels. These systems have been implemented for horizontal excitation, but there has been very limited research on isolation for vertical excitation. To this end, a vertical equipment isolation system is proposed which exhibits a stiff-flexible-stiff behavior to capture different performance goals at different levels. The large initial stiffness restricts the displacement under low hazard levels. The flexibility of the second stage limits the acceleration transmitted to the equipment. Finally, the stiffening in the third stage restrains excessive displacement which can result buckling, yielding and impact with the support. To investigate the effectiveness of the proposed system, a stiff piece of equipment is considered on a particular story of a power plant. The vertical design response spectrum is obtained by multiplying the horizontal response spectrum by appropriate period-dependent V/H ratios. A set of 30 triaxial ground motions are selected and scaled to match the design spectra over the period range of interest. Response history analysis of the structure is carried out to obtain floor motions, which are in turn used as the input to investigate the seismic response of the equipment. The maximum isolation displacement and acceleration response spectra at the floor level and atop the equipment isolation level are used to assess the effectiveness of two isolation systems: a linear spring with a linear viscous damper (LSLD) and a nonlinear spring with a linear viscous damper (NSLD). Both systems manage to significantly reduce the seismic accelerations on the equipment, but the multistage vertical system is shown to exhibit superior seismic performance compared to the conventional linear isolation system.

Keywords: Vertical isolation, Adaptive behavior, Multiple performance goals, Equipment protection, Power plants

INTRODUCTION

Despite the effectiveness of traditional isolation in reducing the horizontal seismic response of equipment, conventional seismic isolation systems are stiff in the vertical direction and thus do not reduce the vertical seismic response. To study the vertical response of base-isolated structures, Furukawa et al. [1] carried out an experimental full-scale test of a medical facility at E-Defense showing that the isolation system effectively reduced the horizontal accelerations, but the vertical accelerations were amplified with height, causing notable nonstructural content damage. In a separate full-scale test at E-Defense, Guzman and Ryan [2] observed the vertical peak floor acceleration in an isolated structure was amplified from 2 g at the second floor to 7 g at the roof.

In recent years, there have been a few attempts to provide effective 3D seismic isolation systems. In general, there are two approaches for 3D isolation. The first approach is to isolate both horizontally and vertically the whole structure at the base level. The second approach is to isolate the entire structure at the base level in the horizontal direction only and to vertically (only) isolate specific vulnerable equipment or floors in the structure. Medel-Vera and Ji [3] concluded that the second approach is more appealing because no rocking suppression system is required, there is no coupling between the horizontal and vertical isolation systems, and it may be more practical for maintenance purposes. Additionally, the weight of targeted equipment is very low compared to the entire superstructure, making the implementation of the vertical isolation practically more feasible. As such, the second approach is explored in this research.

Nawrotzki and Siepe [4] investigated an integrated elastic 3D isolation system they labelled Base Control System (BCS), consisting of helical springs and viscous dampers, to protect emergency diesel generators. The springs were flexible in both the horizontal and vertical directions. They showed that the system improved significantly the seismic performance of the equipment. However, they recommended to check the vertical displacement to avoid any damage to the springs. Lee and Constantinou [5] proposed two 3D isolation systems designed for power transformers. The first system was a horizontal–vertical integrated isolation system consisting of coil springs with an inclined linear viscous damper, and the second one was a system which consisted of a TFP system for horizontal isolation and coil springs with a viscous damper within a telescopic

system for the vertical direction. The study concluded that rocking was a concern for the first system, and that the performance of the second system was more effective in attenuating acceleration response. However, the study also cautioned that the second system may become ineffective for certain ground motions. Specifically, when the vertical frequency of the isolation system was 1.5-2.0 Hz, the seismic response remained unchanged or was amplified for ground motions with strong vertical and horizontal components in the 1.5-3.0 Hz range.

Recently, adaptive behavior in horizontal base isolation systems has been proposed to meet multiple objectives under increasing levels of ground motion excitation. The adaptability of these systems is derived from the physical configuration of the systems. The focus of this paper is to investigate the potential benefits of adaptive vertical isolation systems for equipment. To this end, two systems are studied: a linear spring with a linear viscous damper (LSLD) and a nonlinear spring with a linear viscous damper (NSLD). The systems' ability to reduce the acceleration response of equipment in a nuclear power plant (NPP) is evaluated.

STRUCTURE AND ISOLATED EQUIPMENT

The internal structure of an archetype NPP is represented by a simplified 3D lumped-mass stick model [6] which is adapted in OpenSees [7] and SAP2000 [8] for the purposes of this study, as shown in Figure 1. The total mass of internal structure is 50,000 ton. The height of internal structure is 39 m. The model analysis results show that the natural frequencies of the first and second modes are 7.14 Hz (0.14 s) and 7.69 Hz (0.13s), respectively. The tenth mode of the superstructure is 21.14 Hz (0.0473 s) which is the first mode in the vertical direction. Rayleigh damping is used with 5% damping for the first and tenth modes. Further information about the internal structure can be found in [9], who also used the same representative internal structure design and model configuration but adapted it in SAP2000.

The location is assumed to be at the Diablo Canyon NPP site. The prosses outlined in ASCE 43-05 [10] was used to determine the horizontal and vertical uniform hazard curves for a return period of 10,000 years as the design basis earthquake (DBE) for the NPP. Thirty ground motions were selected and scaled in the range from $0.2T_{\text{fixed-base}}$ to $T_{\text{base-isolated}}$. The scale factors for horizontal and vertical direction were considerably different. Figure 2 shows the target spectra and the mean spectra of ground motions in horizontal and vertical direction, respectively. A motor control center (MCC) (Figure 3), which is described as a "very important electrical equipment with low seismic capacity [11]," was selected to be isolated. The mass of the MCC is 360 kg, so it is negligible in comparison to the total mass of superstructure; hence, a decoupled analysis is used to compute the seismic response. It is assumed that the MCC is attached at the location shown in Figure 1. The fundamental frequencies of the MCC in the two horizontal directions and the vertical direction of the equipment are 5.8, 4.8, and 20 Hz, respectively [12]. Bandyopadhyay and Hofmayer [11] carried out experimental tests on MCC and found three failure modes: contact chatter voltage drop-out, change of state of starter auxiliary contact, and change of state of starter main contact. The fragility curve of the form [13]

$$f = \Phi\left(\frac{\ln\frac{a}{\hat{a}} + \Phi^{-1}(Q)\beta_u}{\beta_r}\right) \quad (1)$$

was derived from experimental data, where a is the peak floor vertical acceleration; Φ is the standard normal cumulative distribution function; Q is the confidence level; $\hat{a}$ is the median capacity; β_u is the uncertainty factor, and β_r is the randomness factor. The recommended parameters of the fragility function for these failure modes are presented Table 1. Figure 4 shows the fragility curves of the three failure modes of the MCC. Although these fragility curves are based on a test protocol input motion that is different from the motion the MCC would experience atop the isolation system in this study, they are used herein in the absence of more appropriate fragility information.

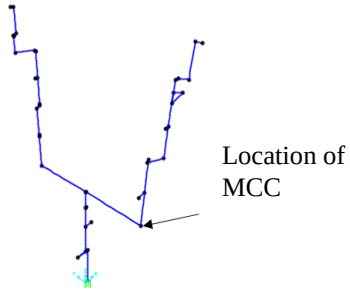

Figure 1: 3D stick model and location of the motor control center

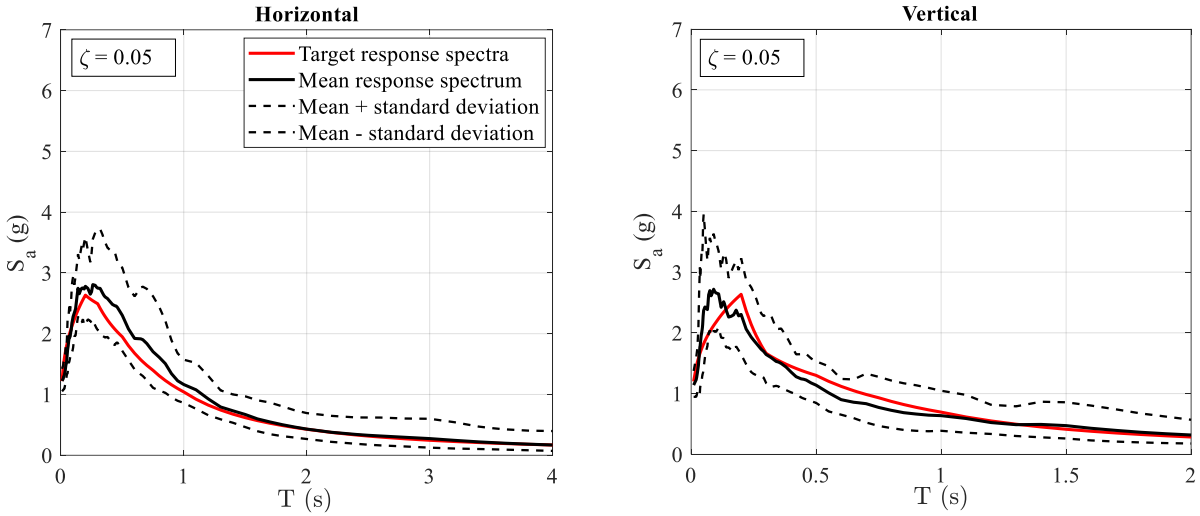

Figure 2: Target and mean response spectra in horizontal (Left) and vertical (right) directions

Figure 3: Schematic view of motor control center [12]

Table 1: MCC failure modes and corresponding fragility parameters

No	Failure Mode	$\hat{a}$	β_u	β_r
1	Contact chatter voltage drop-out	1.3	0.20	0.10
2	Change of state of starter auxiliary contact	1.7	0.17	0.15
3	Change of state of starter main contact	2.1	0.33	0.07

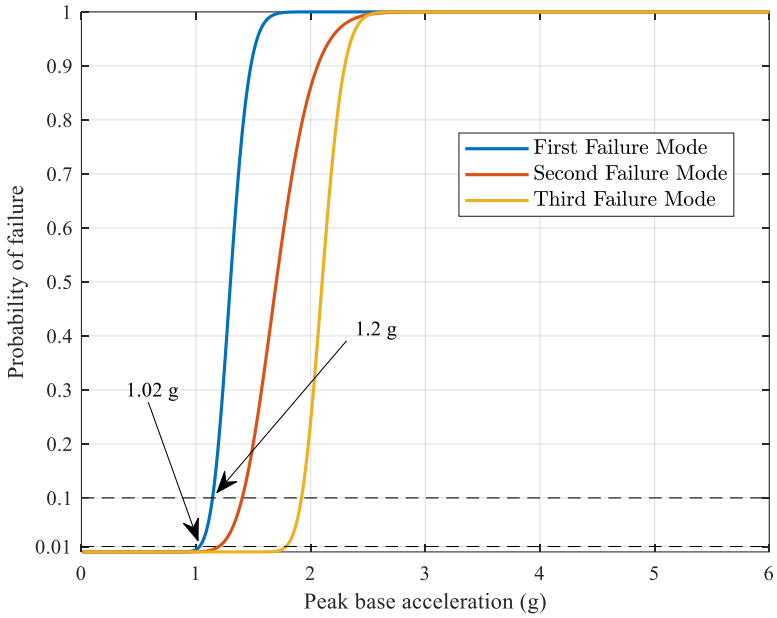

Figure 4: The fragility curves of failure modes of MCC

3D ISOLATION SYSTEMS

A lead rubber bearing (LRB) system was designed for the horizontal isolation at the base of the NPP with effective period and damping ratio of 2.5 s and 0.20, respectively. For the sake of simplicity, the vertical flexibility of the horizontal isolation system was ignored. For the vertical equipment isolation system at the location shown in Figure 1, two systems are explored. The main objective of adaptive isolation systems is to provide protection over a range of seismic hazard levels. To this end, different performance goals are defined under design basis earthquake (DBE) and beyond design basis earthquake (BDBE).

ASCE 43-05 [10] specifies two criteria for structures, systems, and components: (1) They must have less than 1% probability of unacceptable performance for a DBE, and (2) They must have less than 10% probability of unacceptable performance for a BDBE. In addition to the acceleration criteria, there is a maximum possible displacement under BDBE level for the vertical isolation system coming from the displacement capacity of the steel helical springs in compression [14, 15] which is found from

$$u_{max} = \min\left\{u_y = \frac{\tau\pi D^2 n_a}{Gd}, u_b = 0.812l\left(1 - \sqrt{1 - 6.87\left(\frac{2D}{l}\right)^2}\right) when\ \frac{l}{D} > 5.24, u_l = l - nd\right\} \quad (2)$$

where u_y, u_b, and u_l are the yield displacement, buckling displacement, and free length minus solid length of the spring; τ is the permissible shear stress (500~600 Mpa) ; D is the diameter of the spring; n is the total number of coils; n_a is the number of active coils $(n-2)$; G is the shear modulus; d is the diameter of the wire; and l is the free length of the spring. The maximum possible displacement in tension can be defined by using u_y.

The equivalent stiffness and damping for the isolation systems are defined by using the response spectra at the NPP level at which the MCC is attached in conjunction with the fragility curve values given in Table 1. Figure 5 and Figure 6 show the ground response spectra and floor response spectra and displacement spectra under DBE and BDBE level, respectively.

LSLD system

The performance goals for the vertical isolation system are for the probability of contact chatter voltage drop-out (failure mode 1) to remain below 1.02% at the DBE and 10% at the BDBE. Based on the fragility curves in Figure 4, the corresponding accelerations at the base of the equipment are 1.02 g and 1.2 g, respectively. Using the floor spectra corresponding to the location of the MCC (Figure 5, left), an effective frequency of 2.2 Hz and damping of 10% were selected at the DBE level. The

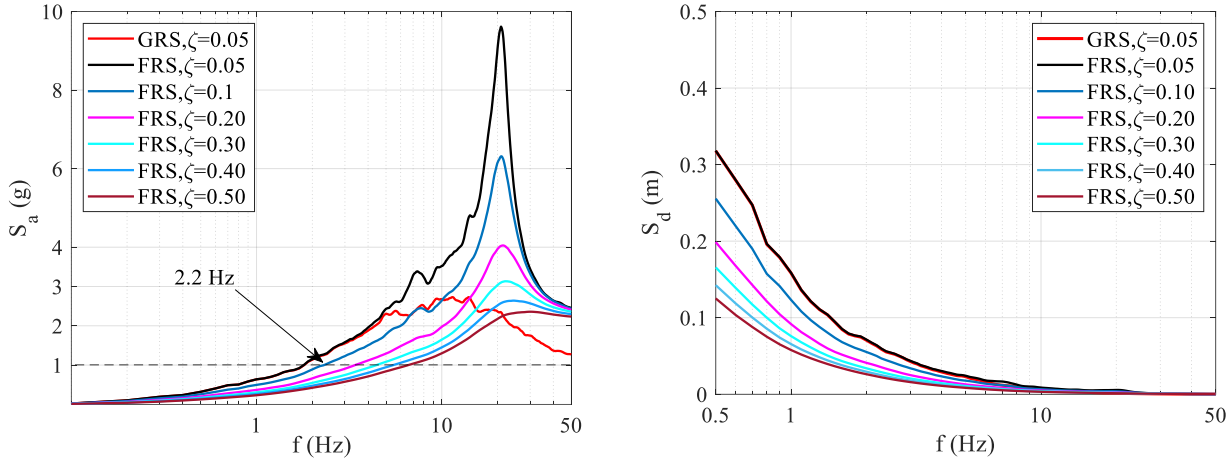

Figure 5: (Left) Acceleration GRS and FRS, and (Right) displacement spectra (all at DBE level)

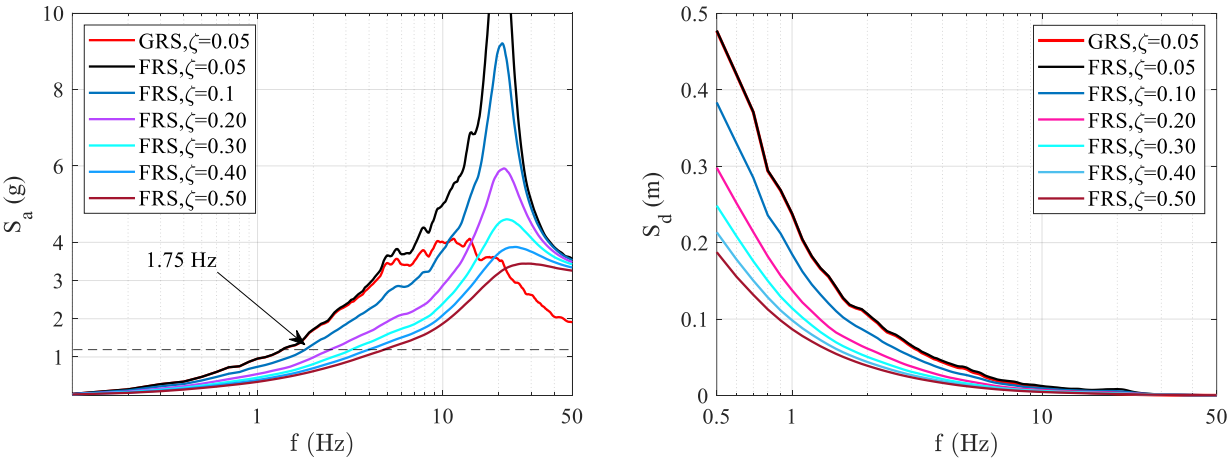

Figure 6:(Left) GRS and FRS and (Right) displacement spectra (all at BDBE level)

corresponding spectral displacement is 0.05 m; and 0.075 m at BDBE. An effective frequency of 1.75 Hz and damping of 10% were selected to meet the goal under the BDBE level. The corresponding displacement demands are 0.07 m and 0.1 m at the DBE and BDBE levels, respectively. The goal under the BDBE level controls the acceleration demands. Consequently, a system with effective frequency of 1.75 Hz and damping of 10% was selected as the accepted LSLD design.

The total displacement demand is the summation of static displacement and dynamic displacement. The static displacement of is dependent on the stiffness of the vertical isolation system and can be computed by:

$$u_s = \frac{g}{4\pi^2 f^2} \tag{3}$$

Figure 7 and 8 show the mean acceleration response spectra, together with the floor response spectra, and the box plots of the maximum displacement of the two LSLD isolation systems at the DBE and BDBE levels. In these figures, the static deflection is shown by a red circle. These figures show that the LSLD system with the frequency 1.75 Hz meets the performance goals under both hazard levels. Table 2 shows four specifications of spring, where *N* is the number of springs. Except for the first specification, the displacement capacity of springs exceeds the displacement demand in all cases.

NSLD system

An effective horizontal seismic isolation system possesses the following characteristics: low mobility during service level conditions, the ability to reduce floor accelerations and interstorey drifts during moderate to strong earthquakes, and the ability to control displacements in extreme earthquakes. These characteristics are achieved by designing an adaptive system that is very stiff at small displacements, yields at low force and becomes flexible for moderate shaking, and stiffens up at large displacements [16, 17]. This strategy is followed for the vertical isolation of the equipment in this research. This behavior is

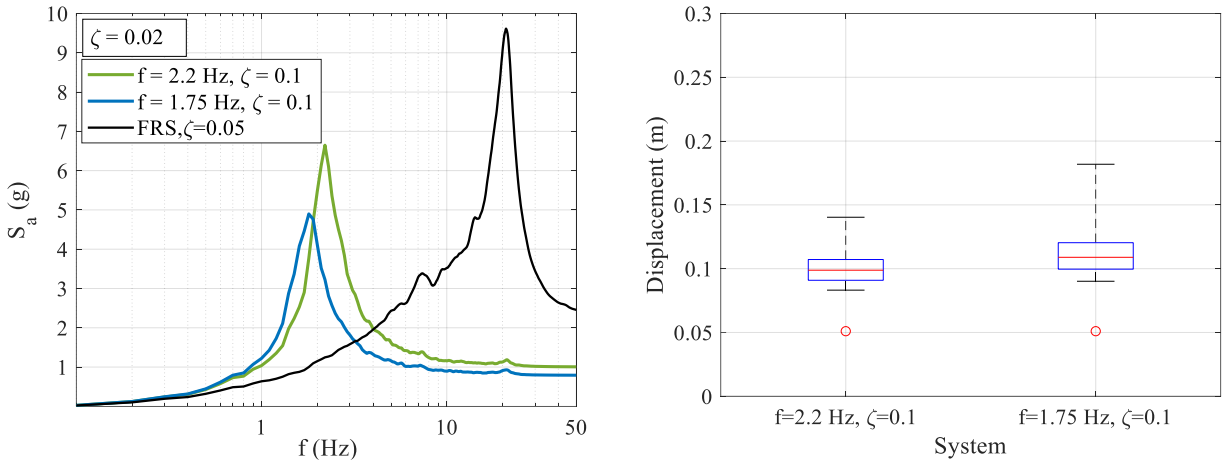

Figure 7: (Left) The mean spectral acceleration and (Right) the boxplot of maximum displacement of isolation system under DBE for the LSLD system. The red circle shows the static displacement.

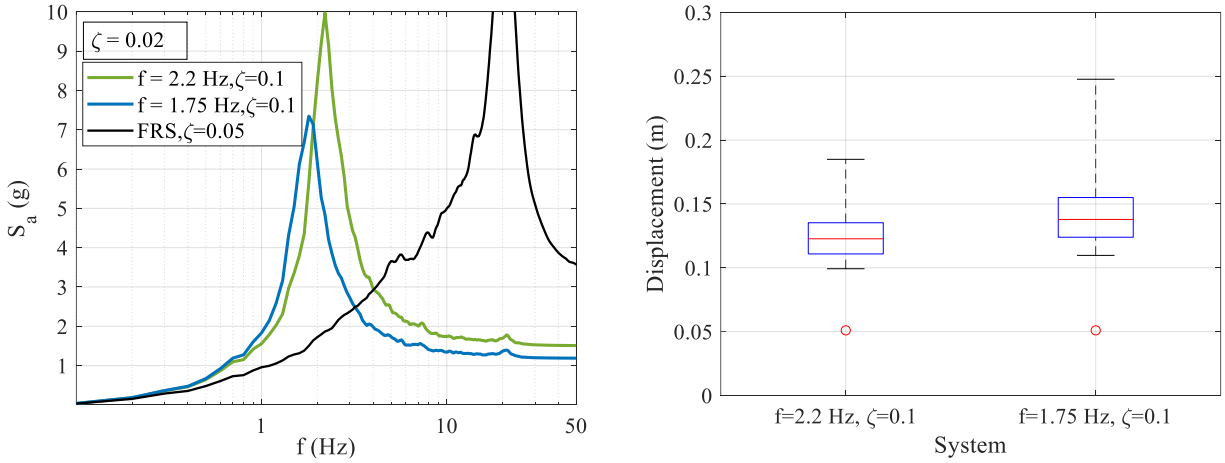

Figure 8: (Left) The mean spectral acceleration and (Right) the boxplot of maximum displacement of isolation system under BDBE for the LSLD system. The red circle shows the static displacement.

Table 2: Four specifications for the springs of the LSLD system with the frequency 1.75 Hz

	N	D(mm)	d(mm)	l(mm)	n	u_y(mm)	l/D	u_b(mm)	u_l(mm)	u_{max}(mm)	u_d(mm)
1	4	105.6	8.6	228	6	141	2.16	-	174	141	150
2	4	107.9	11.1	406	13	259	3.76	-	258	258	150
3	16	33.9	4.1	304	27	153	8.96	259	193	153	150
4	16	49.7	4.5	225	14	168	4.53	-	164	164	150

beneficial to meet the multiple performance objective in different hazard levels. In the case of the NSLD system, the same damping coefficient as that of the LSLD system is used, but the spring is a nonlinear elastic, with three phases up to the BDBE displacement, as shown in Figure 9. F_y is the activation force; K_1, K_2 and K_3 are the stiffness of three phases; d_y is the activation displacement. To achieve an effective stiffnesses of $f_{eff(DBE)}$ at DBE and $f_{eff(BDBE)}$ at BDBE, K_2 and K_3 can be determined from:

$$K_2 = \frac{4\pi^2 m d_{DBE} f_{eff(DBE)}^2 - F_y}{d_{DBE} - d_y} \tag{4}$$

$$K_3 = \frac{4\pi^2 m\left[d_{BDBE} f_{eff(BDBE)}^2 - d_{DBE} f_{eff(DBE)}^2\right]}{d_{BDBE} - d_{DBE}} \tag{5}$$

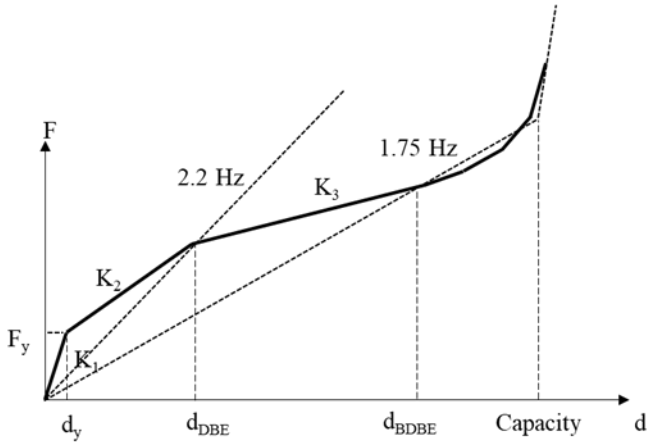

Figure 9: Force-displacement relationship of the elastic nonlinear spring in the NSLD system

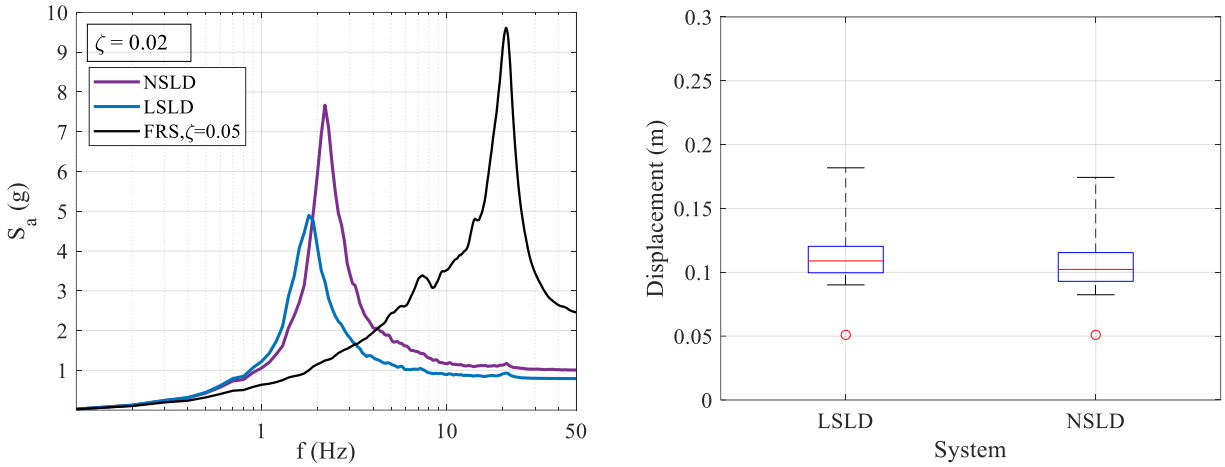

Figure 10: (Left) The mean spectral acceleration and (Right) the boxplot of maximum displacement of isolation system under DBE for the LSLD and NSLD systems. The red circle shows the static displacement.

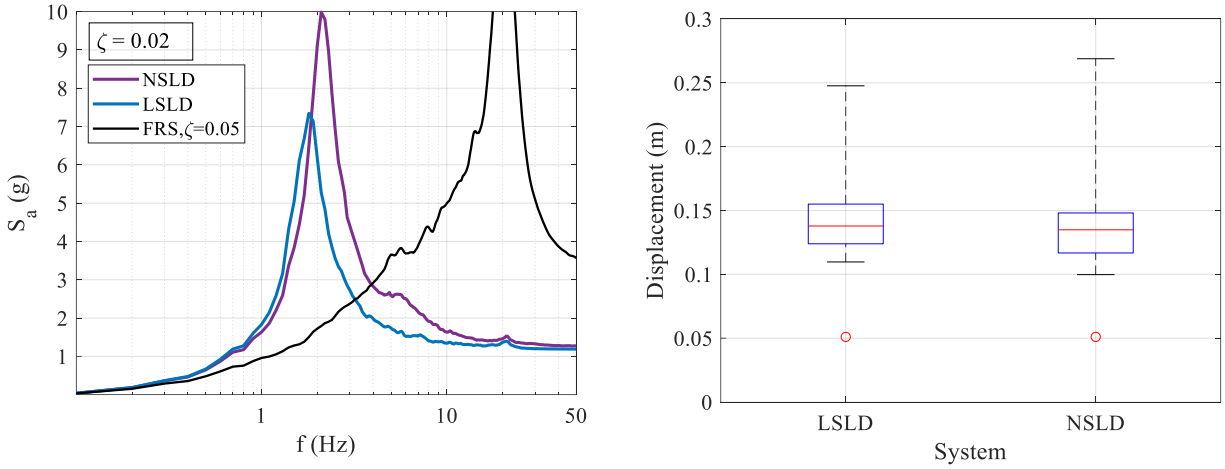

Figure 11: (Left) The mean spectral acceleration and (Right) the boxplot of maximum displacement of isolation system under BDBE for the LSLD and NSLD systems. The red circle shows the static displacement.

where m is the mass of the equipment. The initial stiffness avoids the activation of isolation system for low shaking which may be generated by any type of environmental vibration. The values of F_y and d_y are assumed to be $0.1mg$ and 0.001 m, respectively. The effective frequencies were selected 2.2 Hz and 1.75 Hz under the DBE and BDBE levels. The stiffening at

the large displacement was reserved for large displacement when approaching the capacity of isolation system. This capacity can be considered in nonlinear springs as free length minus the solid length of spring. In opposition to the LSLD system which has a sudden stiffening at capacity displacement, the NSLD system has a smooth stiffening after d_{BDBE}. However, impact was not studied in this research. Figure 10 and 11 compares the spectral acceleration and box plot of displacement of isolation system for the LSLD and NSLD systems. These figures show that the NSLD system can achieve the goals under two hazard levels.

DISCUSSION AND CONCLUSION

This paper investigated the seismic response of two potential vertical isolation systems for acceleration-sensitive equipment in NPPs: a linear spring with a linear viscous damper (LSLD) and a nonlinear spring with a linear viscous damper (NSLD). The study focused on the multiple performance goals under different hazard levels and the capability of adaptive systems to achieve these goals. The fragility function of a motor control center (MCC) was used to identify the performance goals under the DBE and BDBE hazard levels. The performance goal under the BDBE level was used to design the LSLD system. In the case of the NSLD system, the goals under DBE and BDBE levels were used to design the isolation system with different effective characteristics. The result showed that both systems could meet the goals under both hazard levels. However, the effect of initial stiffness and the stiffening for large displacement of the NSLD system was not studied in this research which can be potential advantage of the NSLD system. It is recommended to explore the effect of the stiffening regime in future research.

ACKNOWLEDGMENTS

Financial support for this study was provided by the Natural Science and Engineering Research Council (NSERC) of Canada through the Canadian Nuclear Energy Infrastructure Resilience under Seismic Risk (CaNRisk) – Collaborative Research and Training Experience (CREATE) program at McMaster University.

REFERENCES

[1] Furukawa, S., Sato, E., Shi, Y., Becker, T. and Nakashima, M. (2013). "Full- scale shaking table test of a base- isolated medical facility subjected to vertical motions." *Earthquake Engineering & Structural Dynamics*, 42(13):1931-49.
[2] Guzman, J. and Ryan, K. (2018). "Computational simulation of slab vibration and horizontal- vertical coupling in a full-scale test bed subjected to 3D shaking at E- Defense." *Earthquake Engineering & Structural Dynamics*, 47(2):438-59.
[3] Medel-Vera, C. and Ji, T. (2015). "Seismic protection technology for nuclear power plants: a systematic review." *Journal of Nuclear Science and Technology*, 52(5):607-32.
[4] Nawrotzki, P. and Siepe, D. (2014)."Structural Challanges of power plants in high seismic areas." *Second European Conference on Earthquake Engineering and Seismology*, Istanbul, Turkey.
[5] Lee, D. and Constantinou, M. C. (2018). "Combined horizontal–vertical seismic isolation system for high-voltage–power transformers: development, testing and validation." *Bulletin of Earthquake Engineering*:1-24.
[6] Saudy, A. (2017). Personal Communication. Kinetrics Company.
[7] OpenSees. (2018). Open System for Earthquake Engineering Simulation (Computer software).
[8] SAP2000. (2016). Static and dynamic finite elemets analysis of structures (Computer software).
[9] Huang, Y. N., Whittaker, A. S. and Luco, N. (2010). "Seismic performance assessment of base- isolated safety- related nuclear structures." *Earthquake Engineering & Structural Dynamics*, 39(13):1421-42.
[10] American Society of Civil Engineers - ASCE (2005). *ASCE/SEI 43-05: Seismic Design Criteria for Structures, Systems, and Components in Nuclear Facilities*, USA.
[11] Bandyopadhyay, K. and Hofmayer, C. (1986). *Seismic fragility of nuclear power plant components. Phase I*. Report No. NUREG/CR-465g, BNL-NUREG-52007,Vol.2, Brookhaven National Lab., Upton, NY (USA).
[12] Radford, T. (2015). *Electrical Cabinet Seismic Frequency Estimation.* EPRI Webinar. USA.
[13] Huang, Y.-N., Whittaker, A. S. and Luco, N. (2011). "A probabilistic seismic risk assessment procedure for nuclear power plants:(II) Application." *Nuclear Engineering and Design*, 241(9):3985-95.
[14] Shigley, J. E. (2011). *Shigley's mechanical engineering design.* McGraw-Hill Education. USA.
[15] Becker, L. E. and Cleghorn, W. (1992). "On the buckling of helical compression springs." *International journal of mechanical sciences*, 34(4):275-82.
[16] Fenz, D. M. and Constantinou, M. C. (2008). "Spherical sliding isolation bearings with adaptive behavior: Experimental verification." *Earthquake engineering & structural dynamics*, 37(2):185-205.
[17] Kelly, J. M. (1999). "The role of damping in seismic isolation." *Earthquake engineering & structural dynamics*, 28(1):3-20.